

Structural Variety of Alkali Metal Compounds Containing P–E–M (E = S, Se; M = Li, Na, K) Units Derived from Nitrogen Rich Heterocycles

Jhon A. Balanta-Díaz, Mónica Moya-Cabrera, Vojtech Jancik, Leslie W. Pineda-Cedeño,
Rubén A. Toscano, and Raymundo Cea-Olivares*

Instituto de Química, Universidad Nacional Autónoma de México, Circuito Exterior,
Ciudad Universitaria, 04510 México D.F., Mexico

Received October 13, 2008

The preparation of novel alkali metal chalcogenides supported by multidentate nitrogen rich ligands is reported. Treatment of the ligand precursors $[H\{(4,5-(P(E)Ph_2)_2tz)\}]$ (E = S (**1a**), Se (**1b**)) with organolithium reagents or elemental sodium and potassium in tetrahydrofuran (THF) leads to the isolation of **2–7** in high yields. These compounds were characterized by elemental analysis, IR spectroscopy, mass spectrometry, solution and solid-state multinuclear NMR spectroscopy, and single crystal X-ray diffraction analysis. In the solid state, **2**, **4**, and **5** are dimers that contain bimetallic six-membered (M_2N_4) rings (M = Li, Na). In **3**, the discrete monomer $[Li\{4,5-(P(Se)Ph_2)_2tz\}(thf)_2]$ (tz = 1,2,3-triazole) contains a five-membered CPSeLiN ring which adopts an envelope conformation. The polymeric arrangement $[K\{4,5-(P(S)Ph_2)_2tz\}]_\infty$ in **6** displays different bonding modes based on the hapticity of the ligand upon binding to the potassium atom. In compounds **2–6**, the presence of secondary bonding features the alkali metal chalcogen bonds.

Introduction

Despite the fact that alkali metal chalcogenides are important synthons in the formation of diverse inorganic motifs and versatile organic reagents, relatively less effort has been devoted to the heavier chalcogen–alkali congeners.¹ A long-standing problem in the characterization of chalcogen–alkali complexes stems from their poor solubility, tendency toward aggregation, inherent decomposition, and the formation of amorphous solids.² Since these functionalities serve as single-source precursors to semiconducting metal chalcogenides,³ quantum dots,⁴ gas-phase and in-solution deposition methods of metal chalcogenide films, and useful transfer

reagents,^{5,6} the quest for novel chalcogen–alkali compounds underscores their relevance. The structural chemistry of metal–alkali alkoxides and aryloxides has been widely studied, as opposed to that of their heavier chalcogen congeners.^{2,7} As far as heavier chalcogen–alkali complexes are concerned, the use of multidentate donors such as crown ethers leads to the stabilization of $[M(18-crown-6)(thf)_2][SMes^*]$ (M = Na, K; Mes* = 2,4,6-*t*-Bu₃C₆H₂; THF = tetrahydrofuran) thiolates and the $[Na(18-crown-6)(thf)_2][SeMes^*]$ selenolate.⁸ It was found that these compounds can behave in the solid state as separated or as contact ions. However, in the absence of crown ethers, higher nuclear aggregates of composition, $[(NaSSiPh_3)_6(toluenes)_2]$, $[(KSCPh_3)_6(hmpa)_2(toluenes)_2]$ (hmpa = hexamethylphos-

* To whom correspondence should be addressed. E-mail: cea@servidor.unam.mx. Tel: +52 (55) 56 22 44 66. Fax: + 52 (55) 56 16 22 17.

- (1) Englich, U.; Ruhlandt-Senge, K. *Coord. Chem. Rev.* **2000**, *210*, 135–179.
- (2) Ruhlandt-Senge, K.; Henderson, K. W.; Andrews, P. C. In *Comprehensive Organometallic Chemistry III*; Mingos, D. M. P., Crabtree, R. H., Eds.; Elsevier: Oxford, U.K., 2007; pp 1–65.
- (3) (a) Davies, R. P.; Martinelli, M. G. *Inorg. Chem.* **2002**, *41*, 348–352. (b) Clegg, W.; Davies, R. P.; Snaith, R.; Wheatley, A. E. H. *Eur. J. Inorg. Chem.* **2001**, 1411–1413.
- (4) Davies, R. P.; Francis, C. V.; Jurd, A. P. S.; Martinelli, M. G.; White, A. J. P.; Williams, D. J. *Inorg. Chem.* **2004**, *43*, 4802–4804.

- (5) Bochmann, M.; Song, X. J. *J. Chem. Soc., Dalton Trans.* **1997**, 2689–2692.
- (6) Blake, A. J.; Howdle, S. M.; Poliakoff, M.; Li, W.-L.; Webb, P. B. *J. Chem. Crystallogr.* **1999**, *5*, 547–554.
- (7) Brooker, S.; Edelmann, F. T.; Kottke, T.; Roesky, H. W.; Sheldrick, G. M.; Stalke, D.; Whitmire, K. H. *J. Chem. Soc., Chem. Commun.* **1991**, 144–146.
- (8) Chadwick, S.; Englich, U.; Ruhlandt-Senge, K.; Watson, C.; Bruce, A. E.; Bruce, M. R. M. *J. Chem. Soc., Dalton Trans.* **2000**, 2167–2173.

phoramide), and $[(\text{KSCPh}_3)_6(\text{toluene})_2]$, can be achieved.⁹ Furthermore, during the investigation of the association and aggregation degree in monomers $[\text{Li}(\text{pmdta})\text{STrityl}]$ ($\text{pmdta} = N,N,N',N'',N'''$ -pentamethyldiethylenetriamine, Trityl = CPh_3) and $[\text{Li}(12\text{-crown-4})_2][\text{SMes}^*]$ together with the $[\text{Li}(\text{thf})_2\text{STrityl}]_2$ dimer, it was demonstrated that the size and donor hapticity of the ligands played a key role.¹⁰ In several instances, having hard and soft donor sites in the same ligand resulted favorably in the formation of chalcogen–alkali compounds, and such is the case of $[\{\text{K}(\text{thf})\text{BuN}(\text{Se})\text{P}(\mu\text{-N}^i\text{Bu})_2\text{P}(\text{Se})\text{N}^i\text{Bu}\}\text{K}(\text{thf})_2]_2$.¹¹ Recently, the use of nitrogen rich heterocycles has attracted great attention not only by their remarkable applications (e.g., corrosion inhibitors, components of pharmaceuticals, and high energy materials) but also by being interesting organometallic ligands.² In this regard, the $[\text{H}\{4,5\text{-}(\text{P}(\text{E})\text{Ph}_2)_2\text{tz}\}]$ ($\text{E} = \text{O}, \text{S}, \text{Se}; \text{tz} = 1,2,3\text{-triazole}$) ligands are interesting by virtue of their coordinating ability. For example, five- ($\text{O}-\text{P}-\text{C}-\text{N}-\text{M}$) or seven-membered ($\text{O}-\text{P}-\text{C}-\text{C}-\text{P}-\text{O}-\text{M}$) chelate rings can be attained by the reaction of $[\text{H}\{4,5\text{-}(\text{P}(\text{O})\text{Ph}_2)_2\text{tz}\}]$ with selected transition metals.^{12a} However, in the $[\text{InMe}_2\{4,5\text{-}(\text{P}(\text{E})\text{Ph}_2)_2\text{tz}\}]_2$ ($\text{E} = \text{O}, \text{S}, \text{Se}$) complexes, the central cores contain a bimetallic In_2N_4 unit resulting in a dimeric-like arrangement.¹³ Previously, we have reported on the formation of chalcogen–alkali metal complexes supported by the $\text{HN}[\text{P}(\text{E})\text{Ph}_2]_2$ ($\text{E} = \text{O}, \text{S}, \text{Se}$) ligand and crown ethers.¹⁴ We now turn our attention to the preparation of s-block metal complexes by taking advantage of steric and electronic properties of the triazole-based chalcogen–phosphoranyl ligands that can be an alternative to the P–N–P unit-containing species.¹⁵ Herein, we report the structural variety displayed when lithium, sodium, and potassium centers bind to the nitrogen rich ligand leading to P–E–M ($\text{E} = \text{S}, \text{Se}; \text{M} = \text{Li}, \text{Na}, \text{K}$) moieties and their characterization by spectroscopic techniques and single-crystal X-ray structural analysis.

Experimental Section

General Information. All reactions were performed under a purified dinitrogen atmosphere using standard Schlenk and glovebox techniques.¹⁶ The samples for spectral measurements were prepared in a MBraun Unilab glovebox. The solvents were purchased from Aldrich, purified according to conventional procedures, and freshly distilled prior to use. Compounds $[\text{H}\{4,5\text{-}(\text{P}(\text{E})\text{Ph}_2)_2\text{tz}\}]$ ($\text{E} = \text{S}$

(1a), Se (1b)) were prepared according to the literature procedure.^{12b,c} NMR spectra were recorded on a JEOL ECLIPSE GX 300 instrument, and the ^1H , ^{31}P , ^7Li , ^{23}Na , and ^{77}Se chemical shifts were reported with reference to SiMe_4 , H_3PO_4 (85%), LiCl (1.0 M in D_2O), NaCl (1.0 M in D_2O), and Se_2Ph_2 in CDCl_3 , respectively. Solid-state NMR spectra were recorded on a Varian Unity 300 spectrometer equipped with a 7 mm room temperature probe and Si_3N_4 rotors, and the ^6Li , ^{23}Na , and ^{77}Se chemical shifts were reported with reference to LiCl , NaCl , and Se_2Ph_2 , respectively. IR spectra were recorded on a Bruker Tensor 27 FT-IR spectrometer in the $4000\text{--}400\text{ cm}^{-1}$ range as KBr discs. Mass spectra were obtained on a Bruker Daltonics Esquire 6000 spectrometer by the electrospray ionization (ESI) technique. Elemental analyses (C, H, N) were performed on a CE-440 Exeter Analytical instrument. Melting points were measured in sealed glass tubes and were not corrected.

Preparation of $[\text{Li}_2\{4,5\text{-}(\text{P}(\text{S})\text{Ph}_2)_2\text{tz}\}(\text{thf})_3](\text{THF})$ (2). To a suspension of **1a** (0.20 g, 0.40 mmol) in THF (15 mL) at $-10\text{ }^\circ\text{C}$ was added dropwise a solution of *n*-BuLi (2.0 M in cyclohexane, 0.24 mL, 0.48 mmol). The reaction mixture was allowed to warm up to ambient temperature and stirred for a further 45 min. Filtration of the insoluble materials through Celite afforded a colorless solution that was then reduced to 10 mL and kept at $-10\text{ }^\circ\text{C}$, yielding a white crystalline solid. Yield 0.15 g, 0.12 mmol (60%); mp $170\text{ }^\circ\text{C}$ (decomp). IR $\tilde{\nu}$ ($\text{KBr}/\text{cm}^{-1}$): 649 (P=S), 618 (P–S). ^1H NMR (300 MHz, toluene-*d*₈, $25\text{ }^\circ\text{C}$, TMS): $\delta = 7.74$ (m, 8H, *o*-Ph–H), $\delta = 6.91$ (m, 12H, *m,p*-Ph–H), $\delta = 3.50$ (m, 8H, O–CH₂ (THF)), $\delta = 1.37$ ppm (m, 8H, –CH₂ (THF)). ^{31}P NMR (121.6 MHz, toluene-*d*₈, $25\text{ }^\circ\text{C}$, 85% H_3PO_4): $\delta = 33.5$ ppm. ^7Li NMR (116.8 MHz, toluene-*d*₈, $25\text{ }^\circ\text{C}$, $\text{LiCl}/\text{D}_2\text{O}$ 1.8 M): $\delta = 1.9$ ppm. ^6Li MAS NMR (44.4 MHz): $\delta = 2.2$ ppm. ESI (CH_3OH): (+) *m/z* 514 ($\text{C}_{26}\text{H}_{20}^7\text{Li}_2\text{N}_3\text{P}_2\text{S}_2$), (–) *m/z* 500 ($\text{C}_{26}\text{H}_{20}\text{N}_3\text{P}_2\text{S}_2$). Elem anal. Calcd (%) for $\text{C}_{68}\text{H}_{72}\text{Li}_2\text{N}_6\text{O}_4\text{P}_4\text{S}_4$ (1303.3 $\text{g}\cdot\text{mol}^{-1}$): C 60.5, H 5.6, N 6.4. Found: C 58.5, H 5.2, N 6.0. Unsatisfactory elemental analysis data was obtained as a result of the loss of coordinated THF molecules during the measurement. The data reported represent the average values taken from the different batches measured.

Preparation of $[\text{Li}\{4,5\text{-}(\text{P}(\text{Se})\text{Ph}_2)_2\text{tz}\}(\text{thf})_2]$ (3). Compound **3** was synthesized using the same procedure outlined above for **2** starting from **1b** (0.50 g, 0.84 mmol) and a solution of *n*-BuLi (2.0 M in cyclohexane, 0.5 mL, 1.0 mmol) in THF (15 mL), affording a white crystalline solid. Yield 0.51 g, 0.68 mmol (81%); mp $158\text{ }^\circ\text{C}$ (decomp). IR $\tilde{\nu}$ ($\text{KBr}/\text{cm}^{-1}$): 586 (P=Se), 569 (P–Se). ^1H NMR (300 MHz, C_6D_6 , $25\text{ }^\circ\text{C}$, TMS): $\delta = 7.84$ (m, 8H, *o*-Ph–H), $\delta = 6.90$ (m, 12H, *m,p*-Ph–H), $\delta = 3.50$ (m, 8H, O–CH₂ (THF)), $\delta = 1.33$ ppm (m, 8H, –CH₂ (THF)). ^{31}P NMR (121.6 MHz, C_6D_6 , $25\text{ }^\circ\text{C}$, 85% H_3PO_4): $\delta = 20.7$ ppm. ^7Li NMR (116.8 MHz, C_6D_6 , $25\text{ }^\circ\text{C}$, $\text{LiCl}/\text{D}_2\text{O}$ 1.8 M): $\delta = 2.8$ ppm. ^6Li MAS NMR (44.4 MHz): $\delta = 2.2$ ppm. ^{77}Se (57.2 MHz, C_6D_6 , $25\text{ }^\circ\text{C}$, $\text{Ph}_2\text{Se}_2/\text{CDCl}_3$ 2.0 M): $\delta = -242.2$ ppm (d, $^1J_{\text{Se},^{31}\text{P}} = -723$ Hz). ESI (CH_3OH): (+) *m/z* 674 ($\text{C}_{30}\text{H}_{28}\text{LiN}_3\text{OP}_2^{80}\text{Se}_2$), (–) *m/z* 594 ($\text{C}_{26}\text{H}_{20}\text{N}_3\text{P}_2^{80}\text{Se}_2$). Elem anal. Calcd (%) for $\text{C}_{30}\text{H}_{28}\text{LiN}_3\text{OP}_2\text{Se}_2$ (745.5 $\text{g}\cdot\text{mol}^{-1}$): C 53.5, H 4.2, N 6.2. Found: C 53.3, H 4.6, N 5.8.

Preparation of $[\text{Na}\{4,5\text{-}(\text{P}(\text{S})\text{Ph}_2)_2\text{tz}\}(\text{thf})_2]_2$ (4). To a suspension of **1a** (0.5 g, 1.0 mmol) in THF (25 mL) at ambient temperature was added finely divided sodium (0.025 g, 1.1 mmol), and the mixture was strongly stirred until all the sodium was consumed. The reaction mixture was filtered through Celite, and the volume of the resulting yellow solution was reduced to 10 mL; upon keeping the solution at $-10\text{ }^\circ\text{C}$, a white crystalline solid was obtained. Yield 0.46 g, 0.34 mmol (68%); mp $338\text{ }^\circ\text{C}$ (decomp). IR $\tilde{\nu}$ ($\text{KBr}/\text{cm}^{-1}$): 650 (P=S), 618 (P–S). ^1H NMR (300 MHz, CD_3OD , $25\text{ }^\circ\text{C}$, TMS): $\delta = 7.61$ (m, 8H, *o*-Ph–H), $\delta = 7.28$ (m, 12H, *m,p*-Ph–H), $\delta =$

- (9) Chadwick, S.; English, U.; Ruhlandt-Senge, K. *Organometallics* **1997**, *16*, 5792–5803.
 (10) Ruhlandt-Senge, K.; English, U.; Senge, M.; Chadwick, S. *Inorg. Chem.* **1996**, *35*, 5820–5827.
 (11) Chivers, T.; Krahn, M.; Parvez, M. *Chem. Commun.* **2000**, 463–464.
 (12) (a) Rheingold, A. L.; Liable-Sands, L. M.; Trofimenko, S. *Angew. Chem., Int. Ed.* **2000**, *39*, 3321–3324. (b) Trofimenko, S.; Rheingold, A. L.; Incarvito, C. D. *Angew. Chem., Int. Ed.* **2003**, *42*, 3506–3509. (c) Rheingold, A. L.; Liable-Sands, L. M.; Trofimenko, S. *Inorg. Chim. Acta* **2002**, *330*, 38–43.
 (13) Moya-Cabrera, M.; Jancik, V.; Castro, R. A.; Herbst-Irmer, R.; Roesky, H. W. *Inorg. Chem.* **2006**, *45*, 5167–5171.
 (14) (a) Hernández-Arganis, M.; Hernández-Ortega, S.; Toscano, R. A.; García-Montalvo, V.; Cea-Olivares, R. *Chem. Commun.* **2004**, 310–311. (b) Román-Bravo, P.; López-Cardoso, M.; García y García, P.; Höpfl, H.; Cea-Olivares, R. *Chem. Commun.* **2004**, 1940–1941.
 (15) Silvestru, C.; Drake, J. E. *Coord. Chem. Rev.* **2001**, *223*, 117–216.
 (16) Shriver, D. F.; Drezdon, M. A. *The Manipulation of Air-Sensitive Compounds*, 2nd ed.; McGraw-Hill: New York, 1969.

3.72 (m, 8H, O—CH₂ (THF)), δ = 1.86 ppm (m, 8H, —CH₂ (THF)). ³¹P NMR (121.6 MHz, CD₃OD, 25 °C, 85% H₃PO₄): δ = 31.6 ppm. ²³Na NMR (116.8 MHz, CD₃OD, 25 °C, NaCl/D₂O 1.0 M): δ = -2.5 ppm. ²³Na MAS NMR (116.8 MHz): δ = -15.3 ppm. ESI (CH₃OH): (+) *m/z* 546 (C₂₆H₂₀Na₂N₃P₂S₂), (-) *m/z* 500 (C₂₆H₂₀N₃P₂S₂). Elem anal. Calcd (%) for C₆₈H₇₂N₆Na₂O₄P₄S₄ (1335.5 g·mol⁻¹): C 61.2, H 5.4, N 6.3. Found: C 60.9, H 5.2, N 6.2.

Preparation of [Na{4,5-(P(Se)Ph₂)₂tz}(thf)₂]₂ (5). Compound **5** was synthesized using the same procedure outlined above for **4** starting from **1b** (0.60 g, 0.98 mmol) and finely divided sodium (25 mg, 1.10 mmol) in THF (25 mL), giving a white crystalline solid from a pale green solution. Yield 0.58 g, 0.42 mmol (86%); mp 320 °C (decomp). IR $\tilde{\nu}$ (KBr/cm⁻¹): 587 (P=Se), 570 (P—Se). ¹H NMR (300 MHz, CD₃OD, 25 °C, TMS): δ = 7.62 (m, 8H, *o*-Ph—H), δ = 7.15 (m, 12H, *m,p*-Ph—H), δ = 3.62 (m, 8H, O—CH₂ (THF)), δ = 1.80 ppm (m, 8H, —CH₂ (THF)). ³¹P NMR (121.6 MHz, CD₃OD, 25 °C, 85% H₃PO₄): δ = 22.5. ²³Na NMR (79.3 MHz, CD₃OD, 25 °C, NaCl/D₂O 1.0 M): δ = -2.7 ppm. ²³Na MAS NMR (116.8 MHz): δ = -24.6 ppm. ⁷⁷Se (57.2 MHz, CD₃OD, 25 °C, Ph₂Se₂/CDCl₃ 2.0 M): δ = -239.2 ppm (d, ¹*J*_{Se,P} = -732 Hz). ⁷⁷Se MAS NMR (57.2): δ = -248.2 ppm (d, ¹*J*_{Se,³¹P} = -685 Hz), δ = -321.9 ppm (d, ¹*J*_{Se,³¹P} = -647 Hz). ESI (CH₃OH): (+) *m/z* 642 (C₂₆H₂₀N₃Na₂P₂⁸⁰Se₂), (-) *m/z* 594 (C₂₆H₂₀N₃P₂⁸⁰Se₂). Elem anal. Calcd (%) for C₆₀H₅₆N₆Na₂O₂P₄Se₂ (1378.8 g·mol⁻¹): C 52.3, H 4.1, N 6.1. Found: C 52.0, H 4.7, N 5.9.

Preparation of [K{4,5-(P(S)Ph₂)₂tz}] (6). Compound **6** was synthesized using the same procedure outlined above for **4** starting from **1a** (0.30 g, 0.60 mmol) and finely divided potassium (26 mg, 0.7 mmol) in THF (25 mL), affording a white crystalline solid from an orange solution. Yield 0.26 g, 0.48 mmol (80%); mp 332 °C (decomp). IR $\tilde{\nu}$ (KBr/cm⁻¹): 645 (P=S), 614 (P—S). ¹H NMR (300 MHz, CD₃OD, 25 °C, TMS): δ = 7.66 (m, 8H, *o*-Ph—H), δ = 7.31 (m, 12H, *m,p*-Ph—H). ³¹P NMR (121.6 MHz, CD₃OD, 25 °C, 85% H₃PO₄): δ = 31.6 ppm. ESI (CH₃OH): (+) *m/z* 540 (C₂₆H₂₀KN₃P₂S₂), (-) *m/z* 500 (C₂₆H₂₀N₃P₂S₂). Elem anal. Calcd (%) for C₂₆H₂₀KN₃P₂S₂ (539.6 g·mol⁻¹): C 57.9, H 3.7, N 7.8. Found: C 57.9, H 3.8, N 7.4.

Preparation of [K{4,5-(P(Se)Ph₂)₂tz}(thf)_{0.25}]₂ (7). Compound **7** was synthesized using the same procedure outlined above for **4** starting from **1b** (0.3 g, 0.5 mmol) and finely divided potassium (26 mg, 0.7 mmol) in THF (25 mL), giving white crystalline solid from a pale green solution. Yield 0.28 g, 0.52 mmol (82%); mp 349 °C (decomp). IR $\tilde{\nu}$ (KBr/cm⁻¹): 584 (P=Se), 567 (P—Se). ¹H NMR (300 MHz, CD₃OD, 25 °C, TMS): δ = 7.68 (m, 8H, *o*-Ph—H), δ = 7.27 (m, 12H, *m,p*-Ph—H), δ = 3.72 (m, 1H, O—CH₂ (THF)), δ = 1.82 ppm (m, 1H, —CH₂ (THF)). ³¹P NMR (121.6 MHz, CD₃OD, 25 °C, 85% H₃PO₄): δ = 21.4. ⁷⁷Se (57.2 MHz, CD₃OD, 25 °C, Ph₂Se₂/CDCl₃ 2.0 M): δ = -241.9 ppm (d, ¹*J*_{Se,³¹P} = -730 Hz). ESI (CH₃OH): (+) *m/z* 636 (C₂₆H₂₀KN₃P₂⁸⁰Se₂), (-) *m/z* 594 (C₂₆H₂₀N₃P₂⁸⁰Se₂). Elem anal. Calcd (%) for C₂₆H₂₀KN₃P₂Se₂ (633.4 g·mol⁻¹): C 49.3, H 3.2, N 7.8. Found: C 48.9, H 3.3, N 8.1.

X-ray Structure Determination. Crystals were mounted on nylon loops and rapidly placed in a stream of cold nitrogen, except for compound **1b**, for which the data were collected at 21 °C. Diffraction data for compounds **2–6** were collected at -100 °C. All data were collected from a Bruker-APEX three-circle diffractometer using Mo K α radiation (λ = 0.71073 Å). Structures were solved by direct methods (SHELXS-97)¹⁷ and refined against all data by full-matrix least-squares on *F*².¹⁸ The hydrogen atoms of C—H bonds were placed in idealized positions, whereas the

hydrogen atom from NH moiety in **1b** was localized from the difference electron-density map, and its position was refined with *U*_{iso} tight to the parent atom. The disordered acetone (in the crystal of **1b**) and THF (in the crystals of **2**, **3**, **5**, and **6**) were refined using geometry and distance restraints (SAME, SADI) together with the restraints for the *U*_{ij} values (SIMU, DELU). One of the THF molecules coordinated to the lithium atom in **3** is disordered over three positions (42.9:31.5:25.6). The high occupancies of all three positions suggest partial rotation of the THF in the crystal. The sum of the occupancies was controlled using the SUMP command implemented in the SHELXL program. The close proximity of the third position with its symmetry equivalent (C31B...C31B 2.67 Å) caused the checkCIF program to double the molecular formula. However, the third position is occupied only from 25.6%; thus, in the crystal, it will never be in the proximity of its symmetry equivalent. When the disorder of this molecule was modeled only over two positions, a similar problem appeared only with longer distance (3.01 Å). The THF molecule in **6** is located on an inversion center and is disordered over four positions (two refined).

Results and Discussion

It is noteworthy that, during the preparation of the ligands [H{(4,5-(P(E)Ph₂)₂tz)}] (E = S (**1a**), Se (**1b**)), we were able to determine by X-ray diffraction analysis the molecular structure of the diphenylphosphinoyl acetylene intermediate as well as new types of polymorph structures of **1a** (Figures S1–S3, Supporting Information). As for **1b**, it was further structurally characterized for the first time (vide infra). Compounds **2** and **3** were prepared by the reaction of **1a** or **1b** with *n*-butyllithium under elimination of *n*-butane in THF at -10 °C. The reaction of elemental sodium or potassium with **1a** and **1b** affords compounds **4–7** accompanied by hydrogen evolution as the only byproduct (Scheme 1).

After workup, compounds **2–7** are obtained in high yields as air- and moisture-sensitive colorless crystalline products. Compounds **2** and **3** are soluble in benzene, toluene, and THF but are insoluble in hexanes. In contrast, compounds **4–7** are fairly soluble in methanol, acetonitrile, and DMSO and do not dissolve in solvents such as dichloromethane, toluene, hexanes, and THF. The IR spectra of **4–7** are devoid of N—H stretching vibrations, confirming the deprotonation of the ligands, and they all display vibration bands ascribed to stretching modes for P—E and P=E (E = S, Se). Thus, these findings are in accordance with the electron density delocalization for these types of systems.¹⁹

Electrospray ionization mass spectrometry (ESI-MS) of **2** in methanol exhibits the presence of a peak at *m/z* = 514 corresponding to the isotopic pattern of the bimetallic species C₂₆H₂₀Li₂N₃P₂S₂. In the case of **3**, a peak with the proper isotopic pattern for the monometallic species C₃₀H₂₉LiN₃OP₂⁸⁰Se₂ was observed at *m/z* = 674. In the same manner, the ESI-MS of compounds **4–7** revealed signal aggregates that correlate well either with mono- or bimetallic fragments proper of each compound.

(17) Sheldrick, G. M. *Acta Crystallogr.* **1990**, *A46*, 467–473; SHELXS-97, Program for Crystal Structure Solution.

(18) Sheldrick, G. M. *SHELXL-97, Program for Crystal Structure Refinement*; Universität Göttingen: Göttingen, Germany, 1997.

(19) (a) Silvestru, I.; Haiduc, R.; Cea-Olivares, R.; Zimbrón, A. *Polyhedron* **1994**, *13*, 3159–3165. (b) Hill, M. S.; Hitchcock, P. B.; Smith, N. *Polyhedron* **2004**, *23*, 801–807.

Scheme 1. Preparation of Compounds 2–7

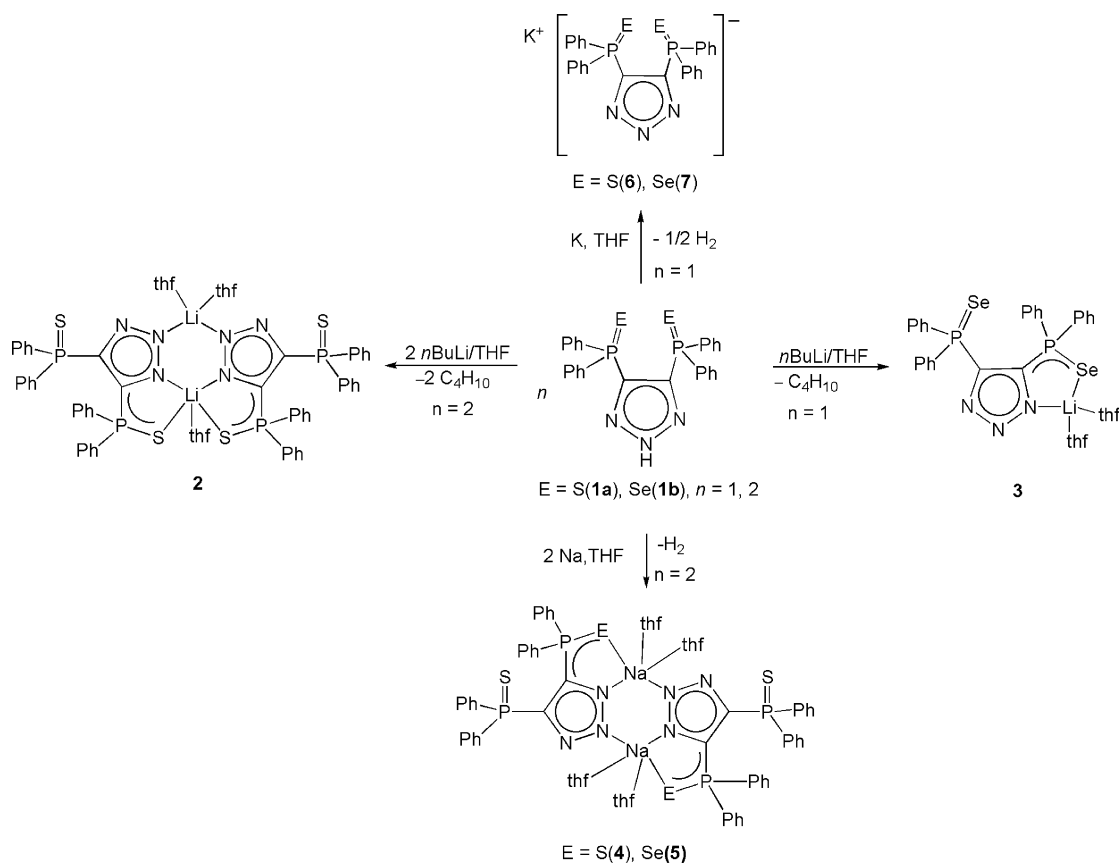


Table 1. Crystallographic Data for 1b and 2–6

	1b	2	3	4	5	6
formula	C ₂₉ H ₂₇ N ₃ OP ₂ Se ₂	C ₆₈ H ₇₈ Li ₂ N ₆ O ₄ P ₄ S ₄	C ₃₄ H ₃₆ LiN ₃ O ₂ P ₂ Se ₂	C ₆₈ H ₇₂ N ₆ Na ₂ O ₄ P ₄ S ₄	C ₆₈ H ₇₂ N ₆ Na ₂ O ₄ P ₄ Se ₄	C ₅₄ H ₄₄ K ₂ N ₆ O _{0.50} P ₄ S ₄
fw	653.40	1303.32	745.46	1335.42	1523.02	1115.27
cryst system	monoclinic	monoclinic	triclinic	triclinic	triclinic	triclinic
space group	C ₂	P2 ₁ /n	P $\bar{1}$	P $\bar{1}$	P $\bar{1}$	P $\bar{1}$
a (Å)	16.139(3)	20.330(4)	9.038(3)	10.577(2)	10.552(2)	13.546(2)
b (Å)	7.437(2)	16.401(3)	11.920(3)	12.779(2)	13.014(3)	13.881(2)
c (Å)	13.696(3)	21.848(4)	16.286(4)	12.988(3)	13.042(2)	15.687(3)
α (deg)	90	90	82.82(4)	75.46(2)	75.75(2)	105.41(3)
β (deg)	116.91(3)	114.99(3)	87.09(3)	78.20(3)	83.16(2)	109.62(2)
γ (deg)	90	90	74.29(3)	82.76(2)	78.23(3)	90.31(2)
V (Å ³)	1466(1)	6603(3)	1676(1)	1658(1)	1695(1)	2664(1)
Z	2	4	2	1	1	2
ρ _{calcd} (g·cm ⁻³)	1.480	1.311	1.478	1.337	1.492	1.390
μ (mm ⁻¹)	2.658	0.294	2.337	0.306	2.324	0.499
F(000)	656	2736	756	700	772	1152
crystal size (mm ³)	0.34 × 0.17 × 0.04	0.30 × 0.21 × 0.12	0.27 × 0.07 × 0.06	0.23 × 0.23 × 0.13	0.21 × 0.15 × 0.13	0.18 × 0.16 × 0.05
θ range for data collection (deg)	2.55 to 25.09	1.15 to 25.10	1.79 to 25.40	1.65 to 25.03	1.62 to 25.39	1.53 to 25.03
no. of reflns collected	6844	35523	16902	20737	18748	26380
no. of indep reflns (R _{int})	2571 (0.0491)	11687 (0.0580)	6122 (0.0709)	5837 (0.0420)	6203 (0.0511)	9412 (0.0709)
no. of data, restraints, parameters	2571, 29, 189	11687, 356, 885	6122, 837, 489	5837, 0, 397	6203, 248, 443	9412, 180, 704
GOF on F ²	0.999	1.023	0.995	1.056	1.013	1.013
R ₁ , wR ₂ (I > 2σ(I))	0.0442, 0.0969	0.0499, 0.1087	0.0531, 0.1010	0.0441, 0.1004	0.0406, 0.0861	0.0569, 0.1154
R ₁ , wR ₂ (all data)	0.0505, 0.1005	0.0686, 0.1180	0.0798, 0.1114	0.0537, 0.1050	0.0554, 0.0922	0.0869, 0.1278
largest diff. peak, hole (e ⁻ ·Å ⁻³)	0.720, -0.252	0.401, -0.272	0.597, -0.470	0.499, -0.210	0.548, -0.317	0.519, -0.368

X-ray Structural Analyses for Compounds 2–6. Colorless single crystals of **1b** and **2–6** were grown from saturated acetone (**1a**) or THF (**2–6**) solutions at -24 °C. However, all attempts for growing single crystals of **7** were unsuccessful. Crystallographic data and refinement details for **1b**

and **2–6** are summarized in Table 1. Selected interatomic distances and angles are provided in Table 2. As outlined before, no structural studies on precursor **1b** have been reported so far. Compound **1b** crystallizes in the monoclinic space group C_2 with one-half of the molecule and one-half

Table 2. Selected Bond Lengths (Å) and Angles (deg) for **1b** and **2–6**

Compound 1b			
N(1)–N(2)	1.312(5)	N(2A)–N(1)–N(2)	117.1(6)
P(1)–C(2)	1.798(6)	C(2)–P(1)–C(1)	107.6(3)
N(2)–C(1)	1.330(7)	C(2)–P(1)–Se(1)	114.8(2)
P(1)–Se(1)	2.094(1)	C(1)–P(1)–Se(1)	112.5(2)
C(1)–C(1A)	1.425(1)	N(2)–C(1)–C(1A)	107.8(3)
N(1)–H(1)	0.820(1)	N(1)–N(2)–C(1)	103.6(4)
H(1)⋯Se(1A)	2.887(1)	N(1)–H(1)⋯Se(1A)	131.9(3)
N(1)⋯Se(1A)	3.885(5)		
Compound 2			
Li(1)–S(1)	2.659(4)	N(2)–N(3)	1.337(3)
Li(1)–S(3)	2.973(4)	N(4)–Li(1)–N(1)	103.6(2)
P(2)–S(2)	1.944(1)	P(1)–S(1)–Li(1)	94.5(1)
P(1)–S(1)	1.971(1)	N(1)–Li(1)–S(3)	109.8(2)
Li(1)–N(4)	2.102(5)	S(1)–Li(1)–N(4)	143.5(2)
Li(1)–N(1)	2.114(5)	S(1)–Li(1)–O(1)	106.2(2)
Li(1)–O(1)	1.935(1)	N(4)–Li(2)–O(1)	107.7(2)
Li(2)–O(3)	1.932(5)	N(2)–Li(2)–O(2)	111.9(6)
Li(2)–N(5)	2.011(5)	N(5)–Li(2)–O(2)	103.7(5)
Li(2)–N(2)	1.984(5)	O(3)–Li(2)–O(2)	105.7(7)
N(1)–N(2)	1.338(3)		
Compound 3			
Li(1)–Se(1)	2.641(8)	C(1)–N(1)–Li(1)	126.8(4)
P(2)–Se(2)	2.105(1)	P(1)–Se(1)–Li(1)	86.9(2)
P(1)–Se(1)	2.136(1)	N(1)–Li(1)–Se(1)	89.4(3)
Li(1)–N(1)	2.001(1)	N(1)–Li(1)–O(1)	109.5(6)
Li(1)–O(1)	1.901(1)	N(1)–Li(1)–O(2)	111.9(6)
Li(1)–O(2)	1.904(1)	O(1)–Li(1)–O(2)	110.0(9)
		O(1)–Li(1)–O(2)	119.3(4)
Compound 4			
Na(1)–S(1)	3.038(1)	P(1)–S(1)–Na(1)	90.0(1)
P(2)–S(2)	1.950(1)	N(2A)–Na(1)–S(1)	166.9(1)
P(1)–S(1)	1.962(1)	N(1)–Na(1)–O(2)	115.0(1)
Na(1)–N(1)	2.462(2)	N(1)–Na(1)–O(1)	149.6(1)
Na(1)–O(2)	2.324(2)	O(1)–Na(1)–O(2)	93.5(1)
N(2A)–Na(1)–N(1)	91.6(7)	O(2)–Na(1)–S(1)	93.4(6)
Compound 5			
Na(1)–Se(1)	3.120(1)	P(1)–Se(1)–Na(1)	87.6(1)
P(2)–Se(2)	2.104(1)	N(2A)–Na(1)–Se(1)	166.7(1)
P(1)–Se(1)	2.117(1)	N(1)–Na(1)–O(2)	114.3(1)
Na(1)–N(1)	2.485(3)	N(1)–Na(1)–O(1)	150.2(2)
Na(1)–O(1)	2.375(4)	O(1)–Na(1)–O(2)	93.2(1)
N(1)–Na(1A)–N(2A)	91.5(1)		
Compound 6			
K(1)–S(1A)	3.343(2)	K(2)–N(5)	2.789(3)
P(2)–S(2)	1.950(1)	K(2)–N(4A)	2.792(3)
P(1)–S(1)	1.960(1)	N(1A)–K(1)–N(1)	88.9(1)
K(1)–N(1)	3.256(3)	P(1)–S(1)–K(1A)	82.7(1)
K(1)–N(2)	2.746(3)	N(2A)–K(1A)–N(1A)	23.8(1)
K(1)–N(1A)	2.787(3)	N(6)–K(1)–N(5)	24.2(2)
K(1)–N(5)	3.216(3)	N(3)–K(2)–C(21)	52.6(1)
K(1)–N(6)	2.722(3)	C(2)–N(3)–K(2)	152.6(2)
K(2)–N(2)	3.200(3)	C(2)–P(2)–C(21)	102.1(2)
K(2)–N(3)	2.706(3)	P(2)–C(21)–K(2)	112.8(1)
K(2)–N(4)	3.280(3)		

of acetone in the asymmetric unit. In **1b**, the triazole ring is planar, and the P–C (1.815(5) Å) and P–Se (2.094(1) Å) bond lengths are in agreement with similar types of compounds.¹⁵ Furthermore, the presence of intermolecular hydrogen interactions N–H⋯Se (N⋯Se, 3.885(5) Å; H⋯Se, 2.886 Å) results in a 1D framework with three-centered hydrogen bonds (Figure 1).

Compounds **2–5** form discrete monomer and dimer structures, while in the case of **6**, a polymeric arrangement was observed. Compound **2** crystallizes in the monoclinic space group $P2_1/n$ with one molecule of **2** and one molecule of THF in the asymmetric unit. The core of **2** consists of a six-membered ring (Li₂N₄) that is fused with four five-

membered rings (two C₂N₃ and two CPSLiN), where the latter are formed by the chelation of the lithium atom to the sulfur and nitrogen atoms (Figure 2). On the basis of the formation of this core, the coordination environments of the two lithium atoms are not equal. The Li(1) atom coordinates to two N atoms and two S atoms from two ligand fragments, while a THF molecule occupies the fifth coordination site. The geometrical arrangement in this metal center is highly distorted, and therefore, Addison and Nageswara's method was used to calculate the degree of trigonal distortion.²⁰ The calculated τ value for Li(1) is 0.44, signifying that the geometry lies between the pathway of a square based pyramid and a trigonal bipyramid. On the other hand, the Li(2) atom binds to two N atoms from two triazole rings and two THF molecules, displaying a tetrahedral arrangement. The Li–S bond lengths with 2.293(4) and 2.659(4) Å are significantly different, although comparable to that in [LiSP(NiPr)(NH₂Pr)₂(thf)] (2.526(4) Å)²¹ as well as in those containing five-coordinate lithium atoms: [Li(tmeda)]₂–[Zr(SC₆H₄-4-Me₃)₆] (tmeda = *N,N,N',N'*-tetramethylenediamine, 2.643 and 2.810 Å)²² and [LiN(C₆H₄SC)(S)(pmdta)] (2.730 Å).²³

Compound **3** crystallizes in the triclinic space group $P\bar{1}$ with one molecule in the asymmetric unit. The geometry around the lithium atom in **3** can be described as a tetrahedron with the lithium atom being surrounded by nitrogen and selenium atoms from the ligand and two coordinating THF molecules forming a five-membered CPSeLiN ring. The ring adopts an envelope conformation with the Li(1), N(1), C(1), and P(1) atoms slightly deviated from planarity and the selenium atom in the out-of-plane position (Figure 3).

The Li–Se bond length (2.641(8) Å) in **3** correlates well with those found in [Li₃(SeP(NPh)₃)(thf)₄]{LiSe(thf)}₂ (2.59(1)–2.71(2) Å).²⁴

Compounds **4** and **5** are isomorphous and crystallize in the triclinic space group $P\bar{1}$ with one-half of the molecule in the asymmetric unit. The bimetallic Na₂N₄ rings in **4** and **5** (Figures 4 and 5) contain two five-coordinated sodium atoms. In terms of the percentage of trigonal distortion ($\tau = 0.29$ and $\tau = 0.28$), each sodium atom in **4** and **5** possesses a square pyramidal geometry. In both cases, the apical position is occupied by the O(2) atom, while the O(1), N(1), N(2A), and E(1) (E = S, Se) atoms take up the basal position. So far, there is just one known example of a five-coordinate sodium atom with a Na–S(P) unit.²⁵ The Na–S bond length in **4** (3.038(1) Å) is larger than those in the P–N–P parent

(20) (a) Addison, A.; Nageswara, T. *J. Chem. Soc., Dalton Trans.* **1984**, 1349–1356. (b) McLanchlan, G. A.; Fallon, G. B.; Martin, R. L.; Spiccia, L. *Inorg. Chem.* **1995**, *34*, 254–261. (c) Muetterties, E. L.; Guggenberger, L. *J. Am. Chem. Soc.* **1974**, *94*, 1748–1756.

(21) Chivers, T.; Krahn, M.; Parvez, M.; Schatte, G. *Chem. Commun.* **2001**, 1922–1923.

(22) Friese, J.; Krol, A.; Puke, C.; Kirstin, K.; Giolando, D. *Inorg. Chem.* **2000**, *39*, 1496–1599.

(23) Andrews, P.; Koutsantonis, G.; Raston, C. *J. Chem. Soc., Dalton Trans.* **1995**, 4059–4065.

(24) Chivers, T.; Krahn, M.; Schatte, G.; Parvez, M. *Inorg. Chem.* **2003**, *44*, 3994–4005.

(25) Yang, J.; Drake, J.; Hernández, S.; Rosler, R.; Silvestru, C. *Polyhedron* **1997**, *16*, 4061–4071.

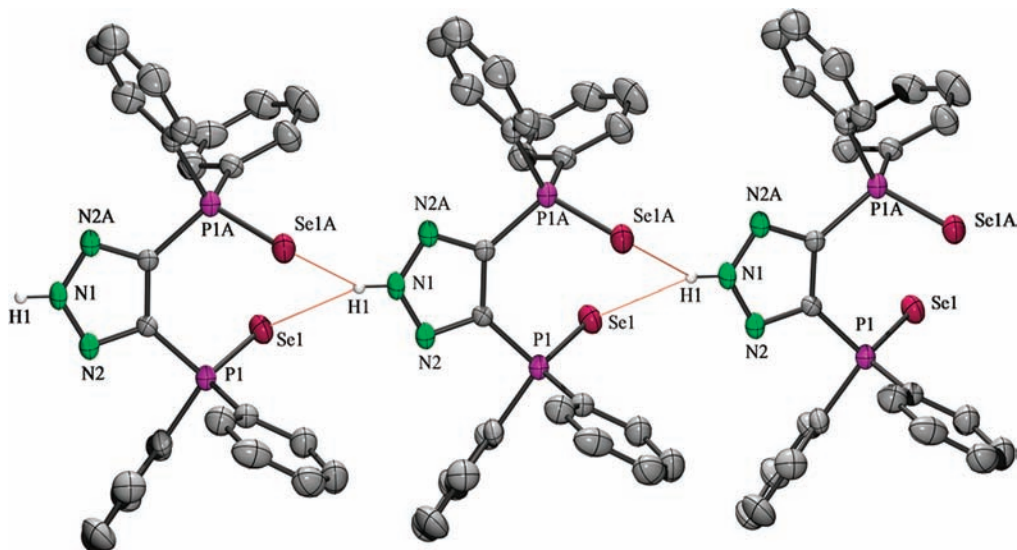


Figure 1. Structural framework of compound **1b** viewing the three-centered hydrogen bonding.

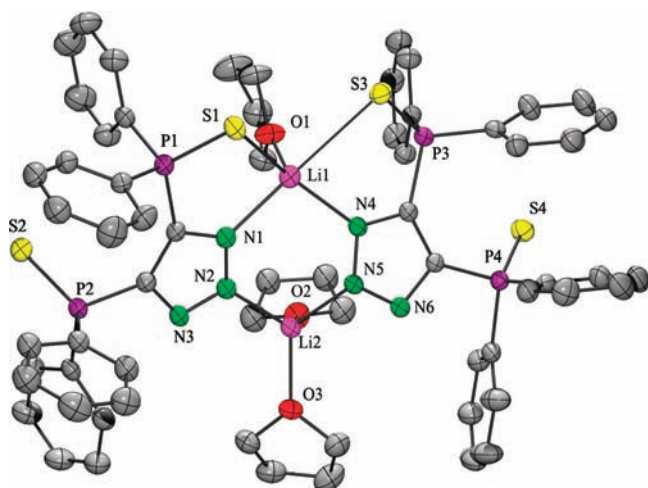


Figure 2. Thermal ellipsoid plot of **2** at the 50% level. Hydrogen atoms are omitted for clarity.

compounds, $[\text{Na}\{(\text{OPPh}_2)(\text{SPPPh}_2)\text{N}\}(\text{thf})_2]_2$ (2.975(6) and 2.790(1) Å)²⁵ and $[\text{Na}\{\text{Ph}_2\text{P}(\text{S})\text{NP}(\text{S})\text{Ph}_2\}(\text{triglyme})]$ (2.884 (2) and 2.841 Å), however, comparable to $[\text{Na}\{\text{Ph}_2\text{P}(\text{S})\text{NP}(\text{S})\text{Ph}_2\}(\text{tetraglyme})]$ (3.084(1) Å).⁶

The Na–Se bond length (3.120(1) Å) in **5** is comparable to those in $[\text{Na}(\text{Ph}_2\text{PSe}_2)(\text{thf})(\text{H}_2\text{O})_5]$ (2.984(1) Å),²⁶ $[\text{Na}_2(\text{PhSe}_2\text{P}-\text{PSe}_2\text{Ph})_2(\text{thf})_3]_\infty$ (3.107(2) Å),²⁷ and $[\text{Na}_2(\text{Se}_3\text{-PPh})(\text{thf})_3]_\infty$ (2.929(2)–3.227(2) Å).²⁸ Further structural analysis of **4** and **5** revealed in both cases chair conformations for the central M_2N_4 cores.

Compound **6** crystallizes in the triclinic space group $P\bar{1}$ with the structural unit of the polymeric chain formed by two $[\text{K}\{4,5\text{-}(\text{P}(\text{S})\text{Ph}_2)_2\}\text{tz}]$ units. In solid state, the two potassium atoms in **6** have different coordination environments, generating 1D polymeric chains (Figure 6). The coordination sphere around the K(1) atom comprises S(1)

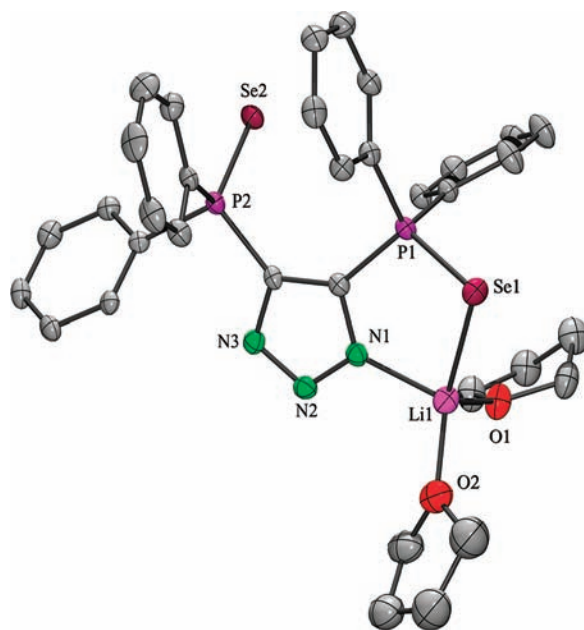


Figure 3. Thermal ellipsoid plot of **3** at the 50% level. Hydrogen atoms are omitted for clarity.

and N(1A) atoms of one ligand segment along with η^2 -phenyl coordination. A second ligand unit is η^2 -bound by N(5) and N(6) atoms and by η^6 -phenyl coordination. The K(1) atom is also linked through N(1) and N(2) atoms in η^2 -contacts by a third ligand fragment.

On the other hand, the K(2) atom exhibits contacts to one ligand unit by the N(4A) and S(3A) atoms and via η^6 coordination of a phenyl ring and η^2 -contacts to N(2) and N(3) atoms from a second ligand unit. A third ligand is coordinated to the K(2) atom by η^2 -bonds to N(4) and N(5) atoms. To our knowledge, these η^1 and η^2 coordination modes for the 1,2,3-triazole ring are unprecedented in any metal system.

The K(1)–S(1A) (3.343(1) Å) and K(2)–S(3A) (3.224(1) Å) bond lengths in **6** are within the range for similar systems exhibiting K–S(P) units.^{27,29} Another aspect of interest in **6** is the presence of phenyl π – π stacking interactions

(26) Pilkington, M. J.; Slawin, A. M. Z.; Williams, D. J.; Woollins, J. D. *Polyhedron* **1991**, *10*, 2641–2645.

(27) Shi, W.; Shafaei-Fallah, M.; Zhang, L.; Anson, C.; Matern, E.; Rothenberg, A. *Chem. Eur. J.* **2007**, *13*, 598–603.

(28) Shi, W.; Shafaei-Fallah, M.; Anson, C. E.; Rothenberger, A. *Dalton Trans.* **2006**, 2979–2983.

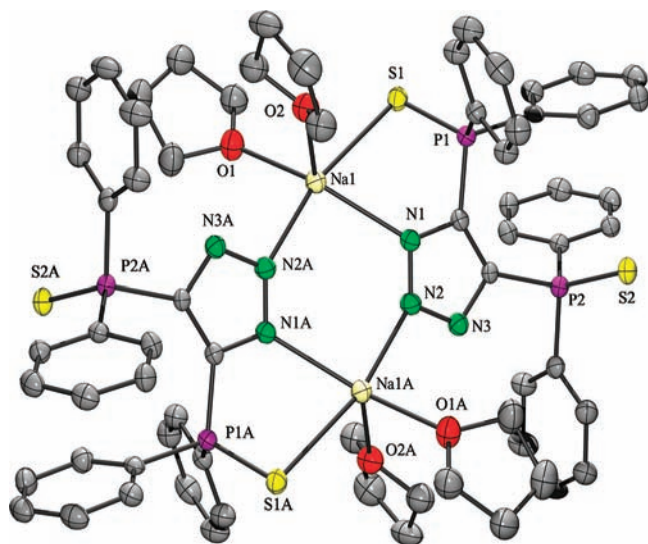


Figure 4. Thermal ellipsoid plot of **4** at the 50% level. Hydrogen atoms are omitted for clarity.

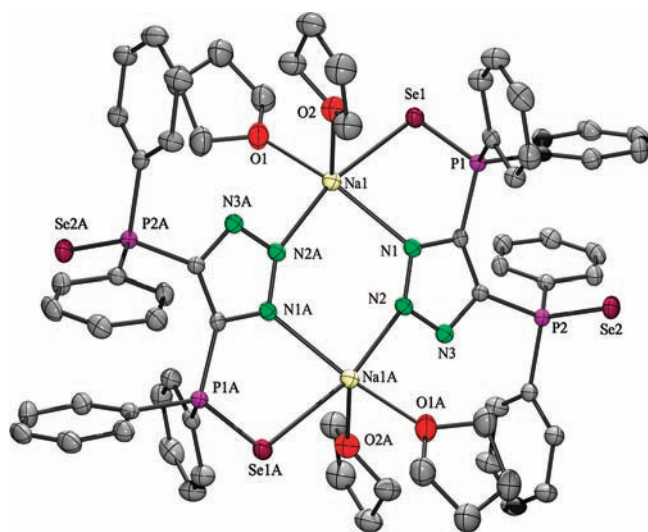


Figure 5. Thermal ellipsoid plot of **5** at the 50% level. Hydrogen atoms are omitted for clarity.

exhibiting different centroid separations (3.62 and 3.74 Å). Furthermore, the inorganic core in the 1D polymer of **6** forms a ladder structure (Figure 7).

The structural arrangements described for compounds **2–6**, namely, the presence of M–E bonding and the M_2N_4 core, are unique structural traits, which are not commonly observed in this or in other azole systems (pyrazole, tetrazole). Only another structurally characterized example of an alkali metal compound comprising a triazole moiety in a M_2N_4 core is known to date,³⁰ while such systems are virtually unknown for tetrazoles. Examples of alkali metals involved in M_2N_4 cores with pyrazole moieties remain scarce. Moreover, in most of these cases, the alkali metals are part of supra-molecular assemblies.

Furthermore, an important implication from the structural data in **2–6** concerns the nature of the chalcogen–alkali

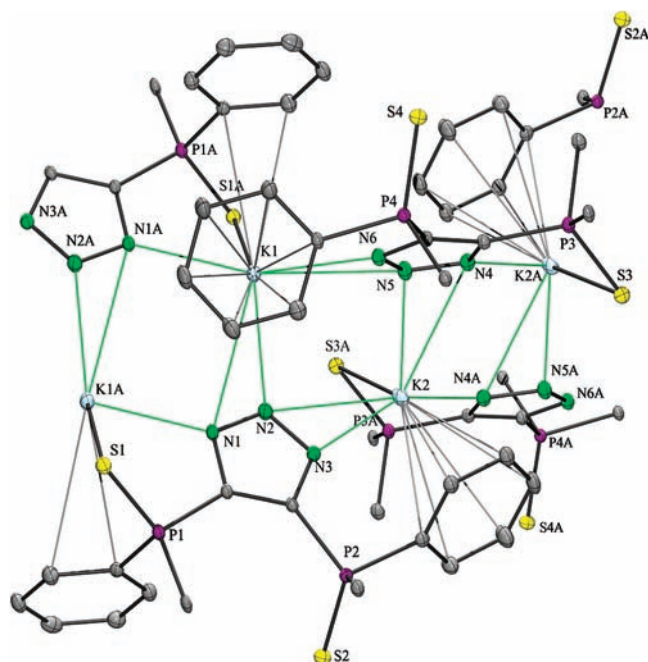


Figure 6. Thermal ellipsoid plot of **6** at the 50% level. H atoms are omitted for clarity.

metal bonding. It was found that the M–E(P) (E = S, Se; M = Li, Na, K) linkage for **2–6** displays somewhat larger chalcogen–alkali interactions than the sum of their covalent radii but is shorter than the Van der Waals radii, thereby falling within the category of secondary bonding. An example for this trend is given by the Li–S bond lengths (2.973(4) and 2.659 Å) in **2**, where these are in average 65% larger than the sum of their covalent radii [$\sum r_{\text{cov}}(\text{Li}, \text{S}) = 1.70 \text{ \AA}$].³⁰ However, in the case of **3**, the Li–Se bond distance (2.641(8) Å) is only 39% larger than [$\sum r_{\text{cov}}(\text{Li}, \text{Se}) = 1.90 \text{ \AA}$].³⁰ The same pattern is observed upon the variation of the chalcogen atoms in **4** and **5**, with 55% larger bond lengths for Na–S and 42% for Na–Se [$\sum r_{\text{cov}}(\text{Na}, \text{E})$: E = S 1.99 Å, E = Se, 2.19].³¹ The shorter bond distances for M–Se with regard to the M–S bonds are the result of the increment of the covalence character of the M–E bonds as the size of the chalcogen increases and size of the metal decreases.³² Indeed, in compound **3**, the small charged lithium atom exerts a greater polarizing effect (relative to sodium or potassium) on the selenium atom, hence increasing the covalent character of the Li–Se bond. The higher covalent character observed in the bonding of **3** contributes to weaker electrostatic interactions with the donor atoms of a second ligand unit, leading consequently to a monomeric structure, as opposed to the M_2N_4 structures observed in the other compounds in this study (**2**, **4**, and **5**). Furthermore, the polymeric nature of compound **6** can be viewed as a token of the higher cationic nature of K^+ and its stronger electrostatic interactions, along with the tendency of form cation π -aromatic interactions.

(29) Ly, T. Q.; Slawin, A. M. Z.; Woollins, J. D. *Angew. Chem., Int. Ed.* **1998**, *37*, 2501–2502.

(30) Boche, G.; Harms, K.; Marsch, M.; Schubert, F. *Chem. Ber.* **1994**, *127*, 2193–2195.

(31) (a) Alcock, N. W. *Inorg. Chem. Radiochem.* **1972**, *15*, 2–53. (b) Bondi, A. *J. Phys. Chem.* **1964**, *68*, 441–451.

(32) Mingos, D. M. P. *Essential Trends in Inorganic Chemistry*; Oxford University Press: New York, 1998; p 43.

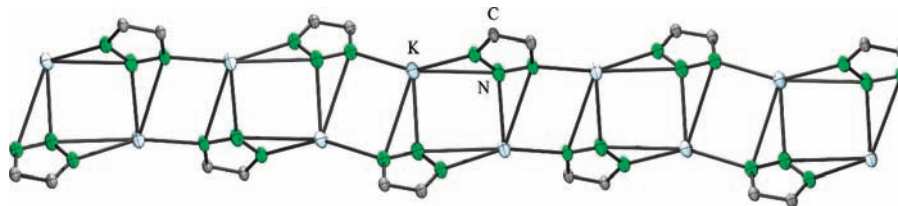


Figure 7. View of the inorganic core of **6** with the ladder structure.

Solution and Solid-State NMR Experiments. After determining the degree of association of **2–6** in the solid state, we became interested in finding out if these associations persist also in solution. Accordingly, multinuclear and low-temperature NMR experiments were carried out on these compounds. In general, it was found that the ^1H NMR spectra of **2–7** show the expected signals for the phenyl groups in the aromatic region. Furthermore, a set of signals for THF molecules, with the exception of **7**, were observed in the ^1H NMR spectra of **2–6**. Interestingly, the ^{31}P NMR spectra of **2** (δ 33.5 ppm), **3** (δ 20.8 ppm), **4** (δ 31.6 ppm), and **6** (δ 31.6 ppm) show a single signal. Indeed, these results are intriguing considering the different coordination environments observed for these compounds in the solid state. Again, the same behavior was seen in the ^{31}P NMR spectra of **5** (δ 22.6 ppm) and **7** (δ 21.4 ppm) but was flanked by Se satellites ($^1J_{^{31}\text{P}-^{77}\text{Se}} = -742$ Hz and -730 Hz, respectively). Furthermore, ^7Li NMR spectra for **2** and **3** exhibit single signals at δ 1.9 and δ 2.8 ppm, respectively. In the case of **3**, one signal is expected as a result of the coordination mode observed in the solid state; nonetheless in **2**, the two distinctive Li atoms should account for two signals. This together with the observation of one sole signal in ^{31}P NMR spectra for **2** and **3** suggests either a dynamic equilibrium or the existence of solvent-separated ion pairs in solution. Accordingly, low-temperature ^{31}P and ^7Li NMR experiments (-80 °C) were performed on **2** and **3** in toluene- d_8 , showing no significant deviation from the trend observed at ambient temperature. Subsequent solid-state ^6Li MAS NMR measurement of **2** revealed one broad peak (δ 2.2 ppm) at a chemical shift similar to the shift observed in solution. Because of the similarity in the chemical shifts of the ^7Li NMR spectrum in solution and in the ^6Li MAS NMR spectrum of **2**, the existence of a very fast dynamic exchange process can be proposed. However, this does not account for the observation of only one signal in solid-state ^6Li MAS NMR. However, the $\text{Li}\cdots\text{Li}$ atom separation in **2** (3.750 Å) is very close to the sum of the van der Waals radii [$\sum r_{\text{vdW}}(\text{Li}, \text{Li}) = 3.64$ Å], therefore enabling the existence of homonuclear dipole–dipole interaction among lithium atoms, which may lead to overlapping signals and, thus, the observation of the broad signal. Furthermore, aside from the single signal observed in the ^{31}P NMR spectrum, the corresponding ^{77}Se NMR spectrum for **3** consists of a doublet centered at δ -242.2 ppm ($^1J_{^{77}\text{Se}-^{31}\text{P}} = -723$ Hz); all of this is consistent with dynamic behavior.

On the other hand, compounds **4** and **5** exhibit one signal in their ^{23}Na NMR spectra at -2.5 ppm and -2.7 ppm, respectively. These chemical shifts are significantly different to those observed in their solid-state ^{23}Na MAS NMR spectra, δ -17.5 and -22.4 ppm for **4** and **5**, respectively. Moreover, in the case of **5**, its ^{77}Se NMR spectrum exhibits one doublet at δ -239 ppm ($^1J_{^{77}\text{Se}-^{31}\text{P}} = -730$ Hz), whereas its ^{77}Se MAS NMR spectrum displays two doublets at δ -248 ($^1J_{^{77}\text{Se}-^{31}\text{P}} = -685$ Hz) and -327 ppm ($^1J_{^{77}\text{Se}-^{31}\text{P}} = -647$ Hz). Considering the differences between the chemical shifts of the solution and those of the solid-state experiments, as well as the fact that methanol- d_4 was used as the solvent for the NMR experiments, we propose the existence of solvent-separated ion pairs for **4** and **5**, promoted by the polar solvent. In the case of compounds **6** and **7**, a similar behavior was found. Further evidence of the presence of solvent-separated ion pairs for **4–7** was obtained by carrying out NMR experiments (^{31}P , ^{23}Na , ^{77}Se) at -80 °C, leading to no significant change regarding the signals observed at ambient temperature.

Conclusion

In summary, alkali metal compounds bearing M–E (M = Li, Na, K; E = S, Se) secondary bonding have been successfully synthesized and structurally characterized. The structural motifs of compounds **2–6** comprise monomeric, dimeric, and polymeric arrangements leading to different ring sizes and geometries. Studies in solution, namely, NMR experiments, suggest a fluxional behavior for compounds **2** and **3**, while for **4–7**, the presence of separated ion pairs is proposed.

Presently, we are studying the reactivity of $[\text{H}\{4,5\text{-}(\text{P}(\text{E})\text{Ph}_2)_2\text{tz}\}]$ (E = S, Se) ligands with selected main group metals, and the outcome of these efforts will be published in due course.

Acknowledgment. We thank the UNAM-DGAPA (Grant IN205208) for financial support. J.A.B.-D. thanks the CONACyT for his Ph.D. fellowship.

Supporting Information Available: Molecular structure of the diphenylphosphinoyl acetylene intermediate, data regarding the new types of polymorph structures of **1a**, and crystallographic information in CIF format. This material is available free of charge via the Internet at <http://pubs.acs.org>.

IC801950Q